A Novel Equation of State for the Prediction of Thermodynamic Properties of Fluids

Ilya Polishuk*,‡ and Juan H. Vera§

Department of Chemical Engineering, McGill University, Montreal, Quebec, Canada H3A 2B2

Received: September 3, 2004; In Final Form: November 22, 2004

This work proposes a new equation of state (EOS) based on molecular theory for the prediction of thermodynamic properties of real fluids. The new EOS uses a novel repulsive term, which gives the correct hard sphere close packed limit and yields accurate values for hard sphere and hard chain virial coefficients. The pressure obtained from this repulsive term is corrected by a combination of van der Waals and Dieterici potentials. No empirical temperature functionality of the parameters has been introduced at this stage. The novel EOS predicts the experimental volumetric data of different compounds and their mixtures better than the successful EOS of Peng and Robinson. The prediction of vapor pressures is only slightly less accurate than the results obtained with the Peng−Robinson equation that is designed for these purposes. The theoretically based parameters of the new EOS make its predictions more reliable than those obtained from purely empirical forms.

1. Introduction

Most of the equations of state (EOS) of practical interest are based on the assumption that the structure of fluids is preliminary determined by short-range repulsive and long-range attractive intermolecular forces. Theoretically based expressions for the repulsive forces, for different molecular shapes, can be tested by comparison with results obtained from Monte Carlo simulations. As a first step, molecules are often considered as hard spheres (HS). In a recent publication, Mulero et al.[1] reviewed 22 analytical expressions that represent the HS virial coefficients and the close-packed limit with different degrees of accuracy. As molecules are usually not spherical, different geometries for hard body (HB) systems have been studied. In particular, some authors[2,3] have proposed HB equations of state to describe the repulsive forces using the expression of Carnahan and Starling.[4] These equations have found wide application for the correlation of computer simulated data.[5] Among other papers dealing with HB-EOS, MacDowell et al.[6] used a modified Wertheim's equation[3] for the description of the compressibility of branched alkanes. However, a significant drawback of the repulsive term of Carnahan and Starling[4] is the inaccurate presentation of the close-packed limit.[7,8] Yelash et al.[9] recently proposed an alternative HB-EOS that yields a more realistic value of the close-packed limit and used this equation for investigation of global phase diagrams of chain molecule mixtures.[10]

Although significant progress has been achieved in the development of theoretically based expressions for hard bodies, those expressions are rarely implemented for the description of phase equilibrium data of real fluids. This is probably due to the inability of thermodynamic models to represent the complexity of the many factors that influence the behavior of real fluids. An improvement in the accuracy of analytical EOS for the modeling of experimental data of real fluids is usually achieved, not by improving their theoretical base, but by introducing empirical temperature functionalities in their parameters.[11,12] Such practice, however, not only hinders the molecular interpretation of results but also diminishes the robustness and reliability of the models.[12−13]

In this study we propose a semitheoretical EOS for the description of experimental data of real fluids, which does not necessarily require implementation of empirical temperature functionalities.

2. Theory

System of Hard Spheres (HS). An appropriate expression for the EOS repulsive term must satisfy two conditions, namely that the compressibility factor, $Z_{rep} = P_{rep}V_m/RT$, tends to infinity at the HS close packed limit[7] and that it gives an accurate representation of the theoretical values of the HS virial coefficients. The simplest expression that satisfies the first condition is given as follows:

$$Z_{rep} = \frac{F(y)}{\left(1 - \frac{6}{\pi\sqrt{2}}y\right)} \tag{1}$$

where y is the packing fraction, that for HS is conveniently written as:

$$y = \frac{b}{4V_m} \tag{2}$$

In eq 2, b is the volume occupied by a mole of hard spheres. Expressions available in the literature use polynomial functions for $F(y)$.[1] Several terms are needed in the polynomial to yield the correct HS close packed limit and properly represent the HS virial coefficients.[7,14] On the other hand, surprisingly accurate results can be obtained from expanding exponential expressions.[15] Considering the simplest possible exponential

* Address correspondence to this author. E-mail: polishyk@bgumail.bgu.ac.il.

‡ Permanent address: the Department of Chemical Engineering & Biotechnology, the College of Judea and Samaria, Ariel, Israel.

§ E-mail: juan.vera@mcgill.ca.

10.1021/jp046025s CCC: $30.25
Published on Web 03/03/2005

TABLE 1: Values of the First Nine Hard Sphere Virial Coefficients

expression	β_2	β_3	β_4	β_5	β_6	β_7	β_8	β_9
theoretical	4	10	18.3648	28.2245 ± 0.0003	39.83 ± 0.38	56.1 ± 2.3	77.0 ± 8.2	98.3 ± 13.1
Carnahan−Starling[4]	4	10	18	28	40	54	70	88
BQ75[8]	4	10	18	28.6667	42.8889	61.8519	87.1358	120.848
eq 3	4.35	10.38	18.5114	28.3742	40.3437	55.4956	75.3793	101.961
eq 4	4	10	18.365	28.5413	40.8466	56.3434	76.6097	103.659

form that yields the correct HS close packed limit we have obtained the following form:

$$Z_{\text{rep}} = \frac{e^{3y}}{\left(1 - \frac{6}{\pi\sqrt{2}}y\right)} \tag{3}$$

However, from the results presented in Table 1 it can be seen that eq 3 fails to yield the exact values for the 2nd and the 3rd HS virial coefficients. Thus, the implementation of additional parameters is unavoidable. After some preliminary trials, we propose the following expression, which satisfies both conditions required from the EOS repulsive term:

$$Z_{\text{rep}} = \frac{e^{\kappa_1 y} - \kappa_2 y - \kappa_3 y^2}{\left(1 - \frac{6}{\pi\sqrt{2}}y\right)} \tag{4}$$

with $\kappa_1 = 3.078$, $\kappa_2 = 0.4285$, and $\kappa_3 = 0.1389$. Table 1 compares the results of the HS virial coefficients from eqs 3 and 4 with the two best repulsive terms expressions available in the literature.[4,8] It can be seen that only eq 4 is able to generate a proper value for the HS third virial coefficient. In addition, the results for the higher HS virial coefficients are also accurate.

System of Hard Bodies (HB). The HS approach is not appropriate for modeling phase behavior of nonspherical molecules. Hence the HS repulsive term given by eq 4 should be modified in order to agree with experimental computer results obtained for hard bodies (HB). This purpose can be achieved by making the value of the packing fraction y and the values of parameters κ_2 and κ_3 dependent on the number of equivalent hard sphere segments (m) in a hard chain molecule. For the packing fraction y, we write,

$$y = \frac{mb}{4V_m} \tag{5}$$

To determine the m-dependencies for κ_2 and κ_3, we have made use of the values of virial coefficients at different reduced site−site densities (L) and m, recently determined by Boublík.[16] A realistic value of L for chain molecules is around 0.5.[16] Thus, from a fit of the virial coefficients of linear hard chain molecules of $L = 0.5$, we obtain:

$$\kappa_2 = 0.6945 - 0.2660m^{5/4} \tag{6}$$

$$\kappa_3 = 0.8404 - 0.7015m^{4/3} \tag{7}$$

Figure 1 compares the values of the 2nd and 3rd virial coefficients from eq 4, using the specializations given by eqs 5−7, with the values determined by Boublík.[15] It can be seen that the agreement is excellent.

However, in practice actual chain molecules can be characterized by motions about bond vectors, which results in stiff bond angles.[17] While extension of the thermodynamic perturbation theory to such complex geometries posses yet unsolved problems, a number of empirical modifications that relate m with the actual number of segments (n) for a more realistic description of flexible chain molecules have been proposed.[18,19] In the present study we adopt the following expression proposed by Yelash and Kraska:[10]

$$m = 1 + 0.377(n - 1) + 0.266\frac{n - 1}{n} \tag{8}$$

For $n = 1$, eq 8 reduces to the case of hard spheres.

System of Interacting Molecules. *A. Hydrocarbon Molecules.* Although experimental data provide an ultimate test of the accuracy of an EOS, distinction should be made between correlation of data and the true prediction. Equations used in engineering practice, such the EOS of Peng of Robinson[20] (PR-EOS), may be used as predictive models for the calculation of vapor pressure data because they have been implemented with generalized empirical temperature functionalities obtained from the correlation of experimental data for the same or similar compounds. Even when the success of this approach is proven by practice, its predictive character is not genuine. As an alternative to this classical engineering EOS approach, it was recently proposed[21] to fit the experimental vapor pressure data by changes in the values of the molecular shape parameters instead of introducing empirical temperature-dependent correlations. It is known[21] that if a van der Waals-like EOS is build using a theoretically based repulsive term, it underestimates the vapor pressure data of spherical and near-spherical compounds. It is not an easy task to develop a van der Waals-like EOS with a theoretically correct HS or HB repulsive term, which could simultaneously give an accurate representation of vapor pressures and densities of real fluids, without making its parameters strongly temperature dependent.

In the present study we propose to minimize this problem by combining a theoretically based repulsive term with corrections for attraction originating from van der Waals and Dieterici[22] potentials. Recently the Dieterici EOS was revisited by

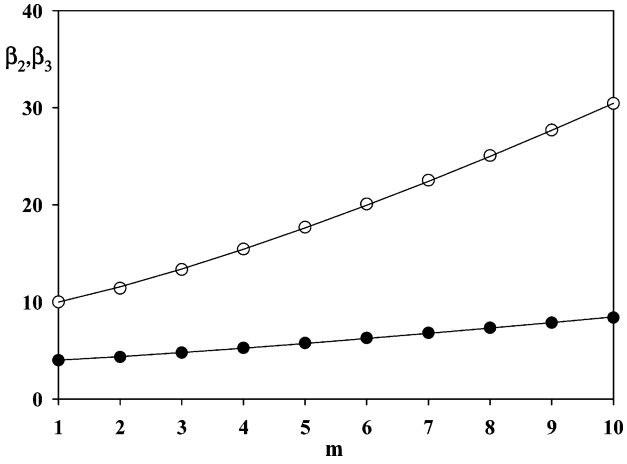

Figure 1. The 2nd and the 3rd HB virial coefficients: solid circles, literature data for the 2nd virial coefficient;[16] open circles, literature data for the 3rd virial coefficient;[16] solid line, results generated by eqs 3−7.

TABLE 2: Values of Ω_a, Ω_b, and Critical Compressibilities for Several *n*-Alkanes

compd	*N*	*m*	Ω_a	Ω_b	$Z_{c,EOS}$	$Z_{c,expt}$ [29]
methane	1	1	0.2585	0.3431	0.3131	0.2862
ethane	2	1.510	0.2925	0.2134	0.3089	0.2792
propane	3	1.931	0.3148	0.1600	0.3057	0.2763
n-butane	4	2.331	0.3332	0.1282	0.3029	0.2739
n-pentane	5	2.721	0.3494	0.1066	0.3002	0.2684
n-hexane	6	3.107	0.3643	0.09095	0.2976	0.2659
n-heptane	7	3.490	0.3783	0.07907	0.2952	0.2611
n-decane	10	4.632	0.4165	0.05613	0.2883	0.2564
n-pentadecane	15	6.526	0.4749	0.03709	0.2774	0.2235
n-hexatriacontane	36	14.45	0.7902	0.01641	0.2300	0.1956

Sadus[23−25] and then further investigated by other authors.[26,27] The practical advantages of combining the van der Waals and the Dieterici potentials into one EOS have been discussed recently.[28] From a more formal point of view, the combination of these two potentials into a single EOS can be interpreted as follows. In a rather unknown publication, MacDougall[29] clearly identified the relation between the van der Waals and the Dieterici approaches. Basically, the hard body pressure, or the hard body compressibility factor, must be reduced due to unbalanced molecular forces close to the surface of the container. Due to the intermolecular potentials holding the molecules together, the external (measurable) pressure is less than that originating from the hard body collisions. van der Waals used the idea of an overall central potential to correct for the wall effects and subtracted a cohesive energy term from the hard core contribution to the pressure. Dieterici, on the other hand, followed a kinetic model in which only molecules having a kinetic energy higher than a certain value could escape the attraction of the bulk fluid to hit the surface of the container. In a generalized form, the Dieterici EOS can be written as

$$P = \frac{RT}{V_m} Z_{rep} e^{-A_c/V_m RT} \tag{9}$$

Notably, an exponential expression for attractive intermolecular interactions is derived from the square-well intermolecular potential and therefore this particular correction has some theoretical background.[30] The important point to note here is that the van der Waals and the Dieterici corrections are not mutually exclusive. Both the overall magnitude of the cohesive energy density and the relative kinetic energy of the molecules can have an effect on the pressure decrease toward the wall of the container. In physical terms, the strength of the intermolecular interactions and the temperature effect, one relative to the other, can affect the measured equilibrium pressure. At low temperature the Dieterici correction factor has a value less than unity and tends to unity as the temperature increases. On the other hand, as proposed by van der Waals, the correction due to the overall central potential is largely independent of temperature. Thus, the general form proposed here is:

$$P = \frac{RT}{V_m} Z_{rep} e^{-A_c/V_m RT} - \frac{a_c}{(V_m + B)^2} \tag{10}$$

where B is a volume displacement parameter and a_c is the typical van der Waals' cohesive energy parameter. An important criterion of the accuracy of EOS is the proximity of their critical compressibility to the experimental values. To fulfill this requirement we have solved the conditions given for the critical

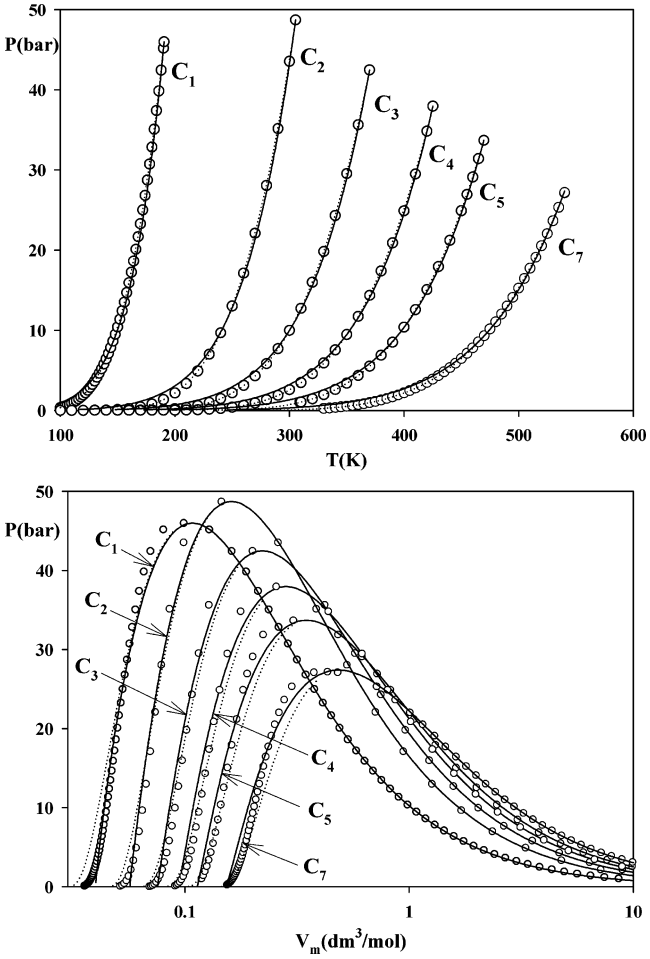

Figure 2. Vapor pressures and molar volumes of light *n*-alkanes: open circles, experimental data for C_1-C_4,[33] C_5,[34] C_7;[35] solid lines, results from eq 10a; dotted lines, data from PR-EOS.

points of pure compounds, namely zero values of the first and second derivatives of pressure with respect to volume, using different values of the EOS parameters. The parameters that yield the desired values of critical compressibility can be generalized as follows:

$$A_c = \frac{7a_c}{4\sqrt{m}} \tag{11}$$

and

$$B = \frac{m^{5/4} b}{4} \tag{12}$$

We note here that A_c and B are temperature independent and depend on structural parameters only. Thus, using eqs 4, 11, and 12, we rewrite eq 10 as:

$$P = \frac{RT}{V_m} \frac{e^{\kappa_1 y} - \kappa_2 y - \kappa_3 y^2}{\left(1 - \frac{6}{\pi\sqrt{2}} y\right)} e^{-7a/4V_m RT\sqrt{m}} - \frac{a}{\left(V_m + \frac{m^{5/4} b}{4}\right)^2} \tag{10a}$$

where the packing fraction y is given by eq 5, $\kappa_1 = 3.078$, and κ_2 and κ_3 are given by eqs 6 and 7, with m given by eq 8. Since the value of m is characteristic of the particular compound, eq 10a is a two-parameter EOS. As in other equations of this kind,

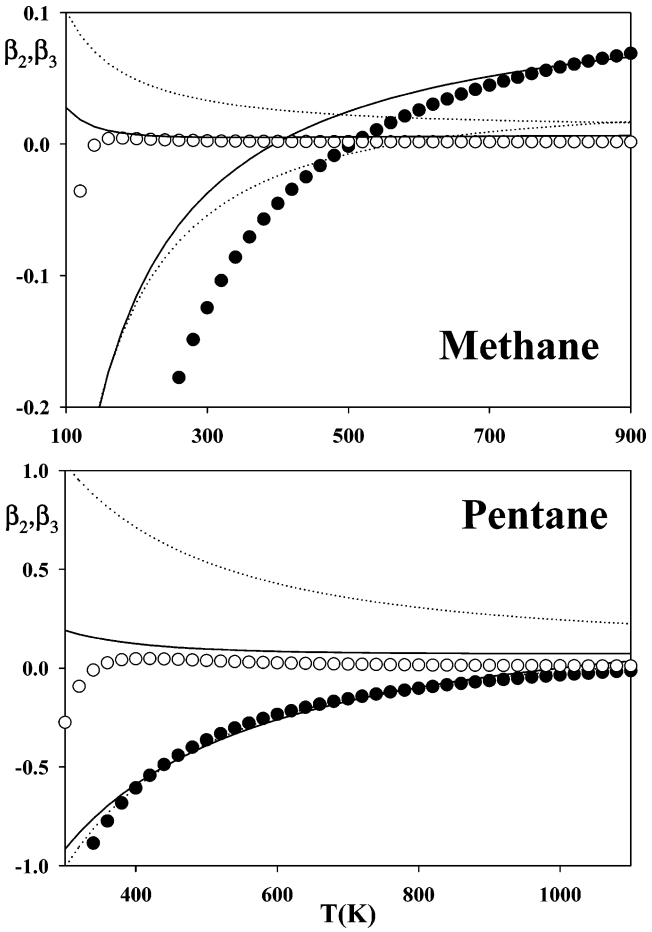

Figure 3. The 2nd and the 3rd virial coefficients of *n*-pentane: solid circles, literature data for the 2nd virial coefficient;[36] open circles, literature data for the 3rd virial coefficient;[37] solid lines, results from eq 10a; dotted lines, results from PR-EOS.

the values of parameters a_c and b are obtained from the relations:

$$a_c = \Omega_a \frac{(RT_c)^2}{P_c} \tag{13}$$

$$b = \Omega_b \frac{RT_c}{P_c} \tag{14}$$

The values of factors Ω_a and Ω_b are evaluated by setting equal to zero the first two derivatives of the pressure with respect to the volume at the critical point. In contrast to ordinary two-parameter EOSs, that by not considering molecular shapes have universal values of Ω_a, Ω_b, and the critical compressibility factor, for eq 10a these factors dependent on the value of m. The values of Ω_a, Ω_b, and critical compressibilities for several *n*-alkenes are listed in Table 2. It can be seen that the values of factors Ω_a and Ω_b from eq 10a for compounds with $n = 7$ to 10 are close to the values typically obtained for engineering cubic EOSs, such as PR-EOS. Important information about the volumetric behavior of eq 10a can be obtained by studying the results shown in Table 2. As already pointed out, eq 10a generates values of the critical compressibility factor which are approximately equal to the experimental values of this parameter.[31] Thus, eq 10a is expected to describe accurately the volumetric properties of both liquid and vapor phases independently of the number of segments in the molecule.

In the above treatment, other than the numerical values of the universal parameters κ_1, κ_2, and κ_3, we have introduced the

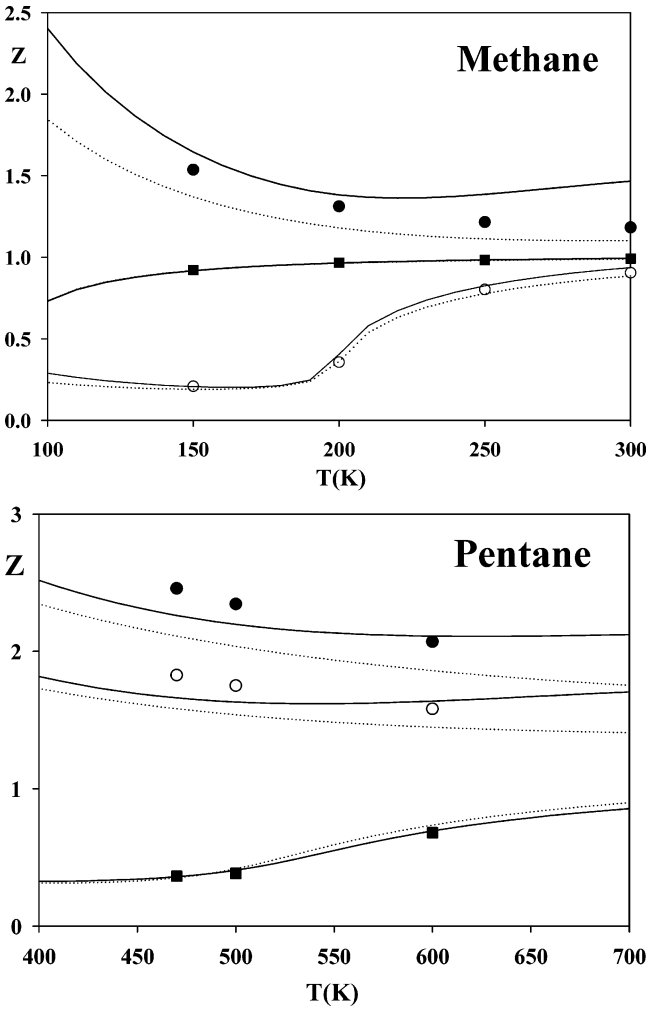

Figure 4. Compressibility of alkanes. Methane: solid circles, 500 atm; open circles, 60 atm; solid squares, 5 atm. *n*-Pentane: solid circles, 700 atm; open circles, 500 atm; solid squares, 80 atm; solid lines, results from eq 10a; dotted lines, results from PR-EOS.

empirical relation of Yelash and Kraska, given by eq 8, and the empirical forms for A_c and B, given by eqs 11 and 12. These later two empirical forms are expected to compensate for the effect of molecular factors not considered by the repulsive−attractive approach. Notably, all the above empirical forms are temperature independent, and the only experimental information used is the volumetric behavior of the fluid at the critical point. Thus, it is interesting to compare the predictive character of eq 10a for volumetric properties and vapor pressures at temperatures other than the critical, with respect to the behavior of typical engineering EOSs such as PR-EOS. For the comparison of prediction of the vapor pressure, however, it is necessary to keep in mind that engineering equations use a temperature-dependent attractive parameter $a = a_c\alpha$, where the generalized function α is obtained from the fitting of vapor pressures. In what follows we compare the ability of both equations to model experimental data of real compounds.

B. Molecules Containing Functional Groups. Implementation of eq 10a is not restricted to *n*-alkanes. It can be expected that the presence of a functional group in a molecule will affect its equivalent hard body parameter m. For practical purposes it would be desirable to have the values of m determined for specific compounds using a group-contribution method. We propose to consider an expression similar to eq 8 in which the addition of each group (CH_3, CH_2, OH, NH_2, etc.) adds one

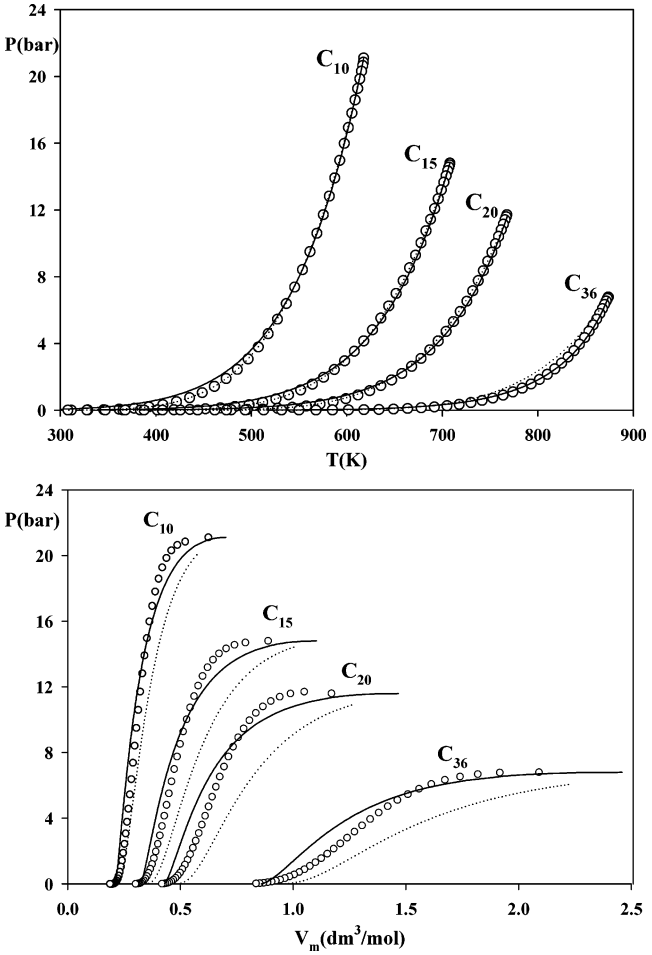

Figure 5. Vapor pressures and molar volumes of heavy *n*-alkanes: open circles, experimental data;[31] solid lines, results from eq 10a; dotted lines, results from PR-EOS.

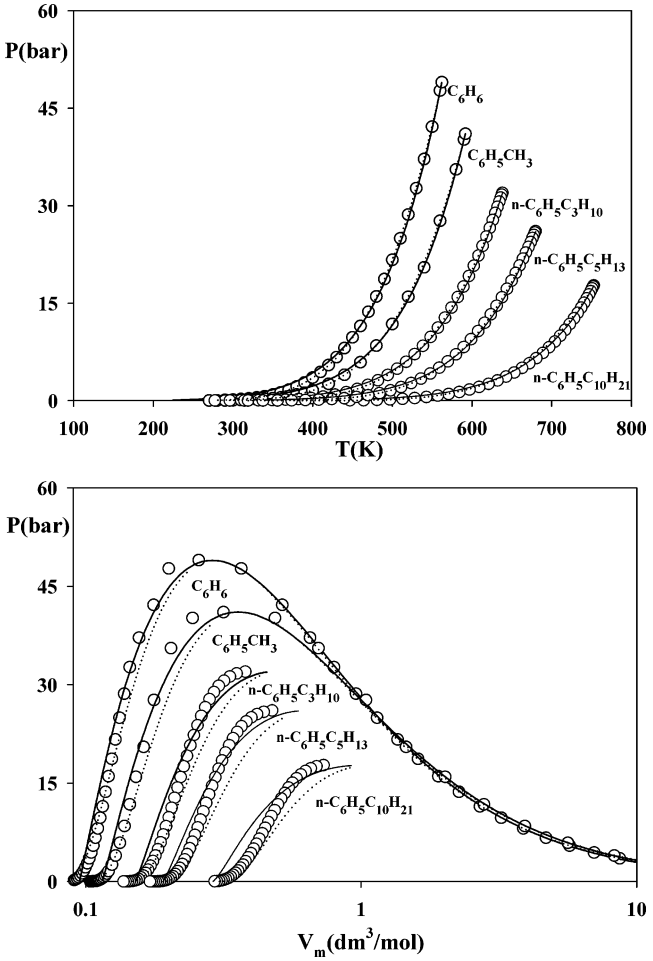

Figure 6. Vapor pressures and molar volumes of benzene and *n*-alkylbenzenes: open circles, experimental data for C_6H_6 and C_6H_5-CH_3[36] and others;[31] solid lines, results from eq 10a; dotted lines, results from PR-EOS.

unit to the value of *n*. In the case of hydrocarbons, for $n = 1$ the equation for hard spheres was recovered. In the case of the first member of a homologous series, this is not expected to be the case. Polar groups usually cause association, which results in the formation of aggregates of different sizes. Hence, the values of *m* of polar groups will be bigger than those for the nonpolar ones. Thus, two factors should contribute to the resulting value of *m* of every particular molecule, namely the chain length and the polarity of its groups. We propose to evaluate the values of *m* for molecules that are omprised of a functional group and the alkane chain by generalizing (8) as:

$$m = m_{\text{group}} + 0.377(n-1) + 0.266\frac{n-1}{n} \qquad (15)$$

For hydrocarbons $m_{\text{group}} = 1$, for *a* homologous series of a particular functional group $m_{\text{group}} \geq 1$. In all cases, *n* just counts the total number of groups in the molecule. The values of m_{group} recommended for the groups considered here are the following: C_6H_5- (C_6H_6), 2.5; OH− (H_2O), 4; and NH_2- (NH_3), 3. A complete development of the group method is considered to be beyond the scope of the present study. It can be seen that a larger value of m_{group} is recommended for a small polar group such as −OH than for the relatively large nonpolar group such as the benzoic ring. These values are justified considering the fact that self-association of water molecules through hydrogen bonds results in the existence of associated structures consisting of even up to 100 monomer units.[38] Thus, the size of aggregates created by the −OH groups is expected to exceed the size of the benzoic ring. In contrast to totally empirical engineering models, the values of parameters used for eq 10a can be supported by molecular arguments.

Treatment of Mixtures. One of the most important applications of EOS is the prediction of the volumetric and thermal behavior of mixtures. Different approaches for mixing rules of the molecular parameters in theoretically based models have been proposed.[12] For the purposes of demonstration, we used here the classical mixing rules:

$$p = \sum_{ij} x_i x_j p_{ij} \qquad (16)$$

where $p = a$, b, and m. The cross-interaction parameters are obtained by using combination rules. For *a* we use:

$$a_{ij} = a_{ji} = (1 - k_{ij})\sqrt{a_{ii}a_{jj}} \qquad (17)$$

For *b* and *m* we use:

$$p_{ij} = p_{ji} = (1 - l_{ij})\frac{p_{ii} + p_{jj}}{2} \qquad (18)$$

Results and Discussion. Figure 2 compares the results from the PR-EOS and eq 10a for vapor pressures and molar volumes of light *n*-alkanes at saturation. It can be seen that the overall

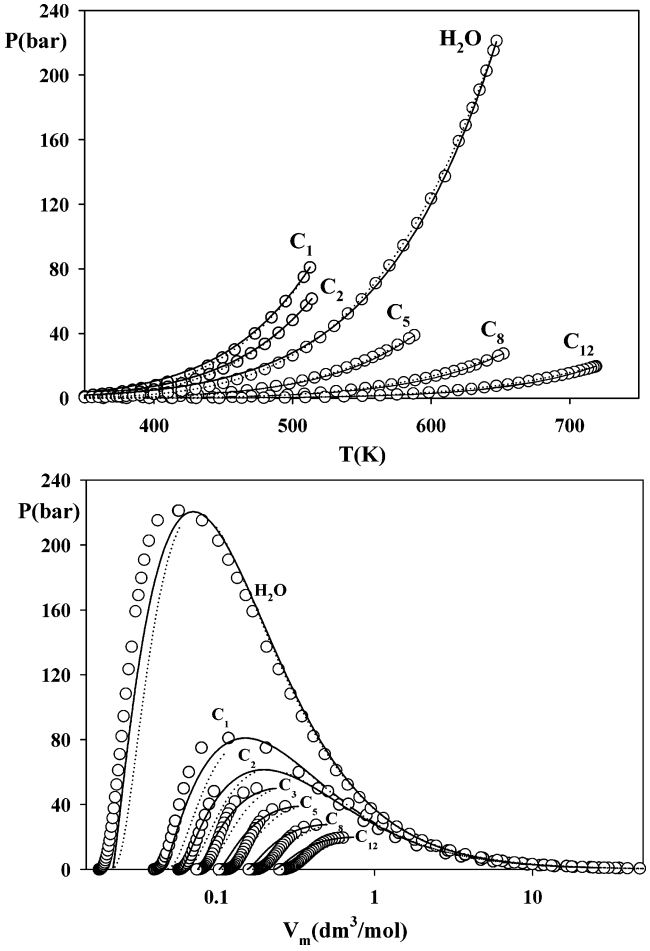

Figure 7. Vapor pressures and molar volumes of water and *n*-alkanes: open circles, experimental data for H_2O, CH_3OH and C_2H_5OH[36] and others;[31] solid lines, results from eq 10a; dotted lines, results from PR-EOS.

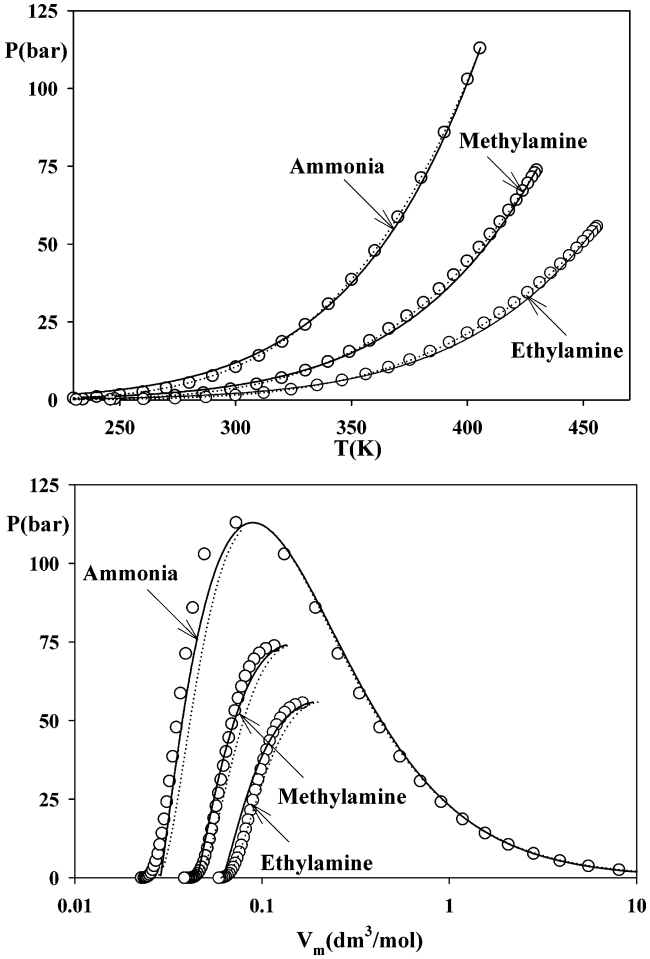

Figure 8. Vapor pressures and molar volumes of ammonia and alkylamines: open circles, experimental data for NH_3[36] and others;[31] solid lines, results from eq 10a; dotted lines, results from PR-EOS.

agreement of both models with experimental data is satisfactory. However, as depicted in Figure 2, the curvature of the vapor pressure lines generated by eq 10a is deficient. This results in a slight overestimation of data in the low-temperature range, where PR-EOS has a certain superiority. It is clear that the accuracy of the latter EOS is achieved thanks to the empirical temperature functionality for the *a* parameter, without which the EOS will fail to describe the data. A similar kind of functionality could be used also for eq 10a, although its numerical contribution is not expected to be significant. Future work will consider the effect of introducing a theoretically based temperature dependence for the *a* parameter in eq 10a.

Figure 2 also shows that both models yield an equally good prediction of the vapor phase volumetric properties of *n*-alkanes. On the other hand, away from the critical point PR-EOS tends to underestimate the liquid molar volume of methane and to overestimate it for *n*-butane and the following homologues. Although eq 10a slightly underestimates these data, it shows a better overall agreement with the experimental values.

Engineering models, such as PR-EOS, usually introduce generalized empirical functionalities fitted to experimental data of vapor pressure and/or saturated molar volumes. Thus, it is of interest to compare the performance of PR-EOS and eq 10a for the prediction of other properties. The ability to predict virial coefficients reflects, in some sense, the accuracy of a model to describe the effect of intermolecular forces. Since engineering cubic EOSs use the inaccurate van der Waals repulsive term, they usually fail in the prediction of the 3rd and higher virial coefficients. However, by a mechanism of cancellation of errors, the results for the compressibility factor are usually satisfactory. Figure 3 presents the results of both models for the 2nd and the 3rd virial coefficients of *n*-pentane. It can be seen that both models accurately predict the 2nd virial coefficient and that the deviations do not exceed the experimental uncertainty. The results for the 3rd virial coefficient are different. In particular, although eq 10a, as other analytical EOSs, does not generate a temperature maximum for this coefficient, it shows a fair agreement with the data. In contrast, PR-EOS fails to represent the 3rd virial coefficient. This failure can be related to the fact that the van der Waals repulsion term significantly overestimates this value. These results demonstrate that in contrast to the PR-EOS, the accuracy of eq 10a is achieved by a better agreement with theory rather than by an error cancellation mechanism.

Figure 4 shows that eq 10a has a clear superiority over PR-EOS for the modeling of the compressibility factor in the superheated region. Both models are in good agreement with data in the vicinity of saturation region, from which the temperature dependence of the PR-EOS *a* parameter was obtained. The deviation from the data of PR-EOS becomes significant at higher pressure. This indicates that the accuracy of PR-EOS in some regions is mostly achieved by an appropriate generalization of the empirical fit of the parameter *a*, and it does not guarantee an accurate description of the behavior of

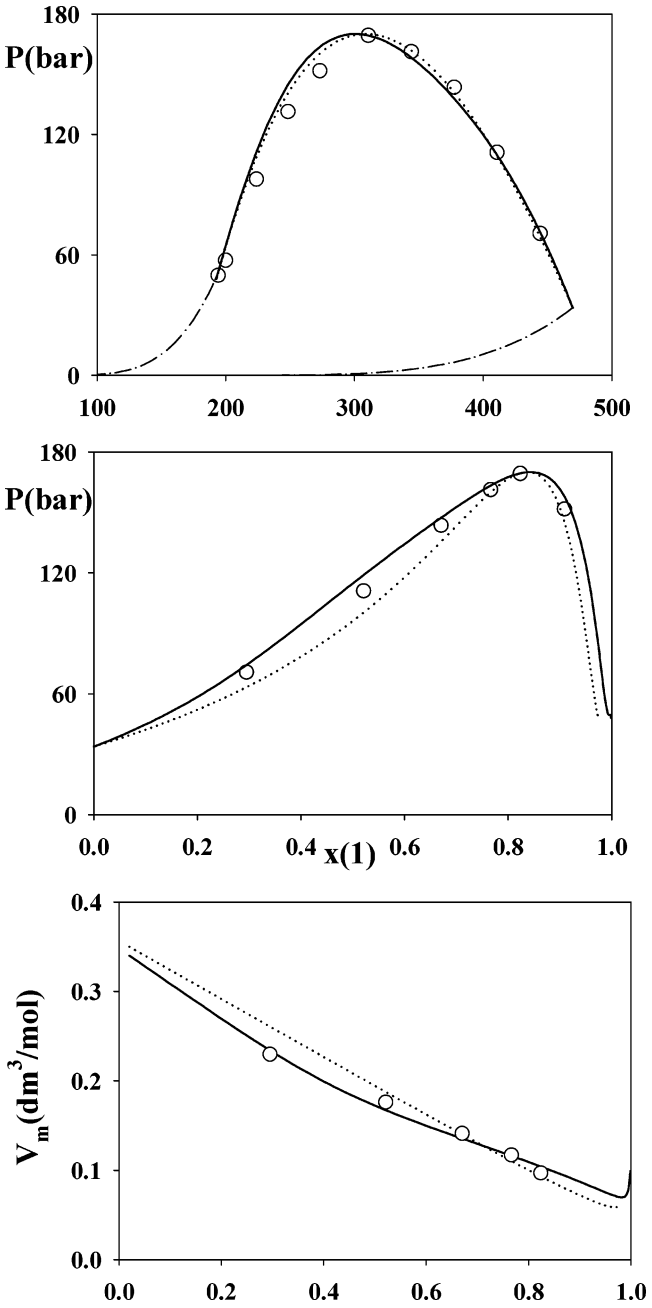

Figure 9. Critical loci of the system methane−*n*-pentane: open circles, experimental data;[39−40] solid lines, results from eq 10a, $k_{12} = -0.16$, $l_{12} = -0.065$; dotted lines, results from PR-EOS, $k_{12} = -0.05$, $l_{12} = -0.03$; dot-dashed lines − vapor pressure curves.

the fluid outside the fitting range. In contrast, the predictions of eq 10a, based only on critical point information, are more reliable.

A similar conclusion is reached analyzing the performance of both models for the case of heavy *n*-alkanes. Figure 5 shows that PR-EOS performs better in the description of the vapor pressure of *n*-decane. However, this superiority tends to disappear with the increase of the chain length of the hydrocarbon. The PR-EOS becomes particularly inaccurate for the prediction of the vapor pressure of *n*-hexatriacontane. This is probably due to the fact that data of heavy hydrocarbons were not included in the temperature fit for the PR-EOS *a* parameter. In contrast, the performance of eq 10a is not affected by an increase of the chain length of the hydrocarbon and the results obtained for the vapor pressure of heavy *n*-alkanes are even better than those for lighter alkanes. The robust characteristics of eq 10a are evident from the molar volume results depicted in Figure 5. In particular, it can be seen that while PR-EOS turns out to be inadequate for the liquid molar volume of *n*-pentadecanene and the heavier homologues, eq 10a yields reasonable predictions of the data.

Figures 6−8 compare predictions of PR-EOS and eq 10a for saturated properties of different compounds. The results show a similar trend to those previously discussed. There is a quite similar accuracy in the description of vapor pressures, with a slight advantage for the PR-EOS results. The superiority of eq 10a is mostly on the prediction of volumetric properties.

Equations 16−18 are probably not the best choice for mixing parameters of the model such as eq 10a and evaluation of the pertinent theoretically based mixing rules will be the subject of a future investigation. Figure 9 presents the critical loci yielded by both models with binary interaction parameters fitted to the pressure and composition of the hypercritical point in the system methane−*n*-pentane. It can be seen that even with the imperfect classical mixing rules, eq 10a shows a clear advantage over the PR-EOS. In particular, in contrast to eq 10a, PR-EOS fails to generate the experimentally observed continuous critical line for this system and presents less accurate modeling in $P - x$ and $V_m - x$ projections. These results again demonstrate the advantage of using a semitheoretical EOS, such as eq 10a, for the modeling of experimental data.

3. Conclusions

The conventional EOS approach for the modeling of fluid phase properties uses empirical temperature functionalities fitted to reproduce the experimental data. Such models can have a predictive character by the use of generalized temperature functions to modify the values of their parameters. Although these models have proven to be successful in practice, normally their parameters have arbitrary values without any molecular justification. As a result, their accuracy is achieved not because of a reliable molecular representation, but due to a cancellation of errors mechanism that does not always work outside the range of the parameter fit.

In the present study we have proposed an alternative approach for predicting experimental data in real fluids, which is based on existing molecular theory. As a first step we have developed a novel simple repulsive term that establishes an exact value of the HS close packed limit and its expansion yields accurate values for the hard sphere virial coefficients. By making this repulsive term dependent on the value of the size of nonspherical hard bodies, a good representation of the values of the hard-chain virial coefficients was obtained. The hard-body model was extended to molecules containing characteristic functional groups. The pressure resulting from the new repulsive term was corrected for the intermolecular attraction effect by terms that combine the van der Waals and Dieterici potentials without empirical temperature functionalities. The resulting equation gives reasonable values of the critical compressibility shift for different compounds.

The novel EOS is able to predict the experimental volumetric data of different compounds and their mixtures better than the successful EOS of Peng and Robinson, but it is slightly less accurate for vapor pressures. These results are achieved by a better molecular thermodynamics basis rather than by an error-cancellation mechanism. This fact makes the predictions of the novel EOS more reliable.

Development of theoretically based mixing rules and the implementation of a group-contribution method for the shape parameters are topics of interest for future research.

Acknowledgment. This work was financed by NSERC Canada.

Appendix A

The fugacity coefficient of a pure compound obtained from eq 10a takes the form:

$$\ln\phi = (Z-1) - \ln Z - \frac{a_c}{RT(V_m+B)} + \left(\frac{\kappa_3 y}{cA_v}\right) \times (1-\exp(-A_v)) + \{E_i[\kappa_1 y - A_v] - \gamma_E - \ln[\kappa_1 y - A_v]\} + \left\{E_i\left[\frac{A_v}{cy} - \frac{\kappa_1}{c}\right] - E_i\left[\left(\frac{A_v}{cy} - \frac{\kappa_1}{c}\right)(1-cy)\right]\right\} \exp\left[-\left(\frac{A_v}{cy} - \frac{\kappa_1}{c}\right)\right] - \left(\frac{\kappa_3}{c^2} + \frac{\kappa_2}{c}\right)\left\{E_i\left[\frac{A_v}{cy}\right] - E_i\left[\left(\frac{A_v}{cy}\right)(1-cy)\right]\right\} \exp\left[-\left(\frac{A_v}{cy}\right)\right] \quad \text{(A-1)}$$

where $A_v = A_c/RTv$, $c = 6/\pi\sqrt{2}$, and $\gamma_E \approx 0.577216...$ is Euler's γ constant and $E_i(X)$ is Euler's exponential integral function defined as:

$$E_i(X) = -\int_{-X}^{\infty} \frac{e^{-t}}{t}\,dt = \gamma_E + \ln|X| + \sum_{k=1}^{\infty} \frac{X^k}{kk!} \quad \text{(A-2)}$$

References and Notes

(1) Mulero, A.; Galán, C.; Cuardos, F. *Phys. Chem. Chem. Phys.* **2001**, *3*, 4991.
(2) Boublík, T. *J. Chem. Phys.* **1975**, *63*, 4084.
(3) Wertheim, M. S. *J. Chem. Phys.* **1986**, *85*, 2929.
(4) Carnahan, N. F.; Starling, K. E. *J. Chem. Phys.* **1969**, *51*, 635.
(5) Sadus, R. J. *AIChE J*. **1999**, *45*, 2454.
(6) MacDowell, L.; Vega, C.; Sanz, E. *J. Chem. Phys.* **2001**, *115*, 6220.
(7) Wang, W.; Khoshkbarchi, M. K.; Vera, J. H. *Fluid Phase Equilib.* **1996**, *115*, 25.
(8) Yelash, L. V.; Kraska, T. *Phys. Chem. Chem. Phys.* **1999**, *1*, 2449.
(9) Yelash, L. V.; Kraska, T.; Müller, E. A.; Carnahan, N. F. *Phys. Chem. Chem. Phys.* **2001**, *3*, 3114.
(10) Yelash, L. V.; Kraska, T. *Phys. Chem. Chem. Phys.* **1999**, *1*, 4315.
(11) Malanowski, S.; Anderko, A. *Modelling Phase Equilibria*: *Thermodynamic Background & Practical Tools*; Wiley: New York, 1992.
(12) Wei, Y.-S.; Sadus, R. J. *AIChE J*. **2000**, *46*, 169.
(13) Segura, H.; Kraska, T.; Mejía, A.; Wisniak, J.; Polishuk, I. *Ind. Eng. Chem. Res.* **2003**, *42*, 5662−5673.
(14) Ghotbi, C.; Vera, J. H. *Can J. Chem. Eng.* **2001**, *79*, 678.
(15) Khoshkbarchi, M. K. Personal communication, 2004.
(16) Boublík, T. *J. Chem. Phys.* **2003**, *119*, 7512.
(17) Flory, P. J. *Statistical mechanics of chain molecules*; Wiley: New York, 1969.
(18) Boublík, T.; Vega, C.; Diaz-Peña, M. *J. Chem. Phys.* **1990**, *93*, 730.
(19) Vega, C.; Lago, S.; Garson, B. *J. Chem. Phys.* **1994**, *100*, 2182.
(20) Peng, D. Y.; Robinson, D. B. *Ind. Eng. Chem. Fundament.* **1976**, *15*, 59.
(21) Polishuk, I.; Wisniak, J.; Segura, H.; Kraska, T. *Ind. Eng. Chem. Res.* **2002**, *41*, 4414.
(22) Dieterici, C. *Ann. Phys. Chem. Wiedemanns Ann*. **1899**, *69*, 685.
(23) Sadus, R. J. *J. Chem. Phys.* **2001**, *115*, 1460; **2002**, 5913 (erratum).
(24) Sadus, R. J. *Phys. Chem. Chem. Phys.* **2002**, *4*, 919.
(25) Sadus, R. J. *Fluid Phase Equilib.* **2003**, *212*, 31.
(26) Bumba, J.; Kolafa, J. *Phys. Chem. Chem. Phys.* **2004**, *6*, 2301.
(27) Polishuk, I.; González, R.; Vera, J. H.; Segura, H. *Phys. Chem. Chem. Phys.* **2004**, in press.
(28) Polishuk, I.; Vera, J. H. *AIChE J.* **2004**, in press.
(29) MacDougall, F. H. *J. Am. Chem. Soc.* **1916**, *38*, 528.
(30) Christoforakos, M.; Franck, E. U. *Ber. Bunsen-Ges. Phys. Chem.* **1986**, *90*, 780.
(31) Daubert, T. E.; Danner, R. P.; Sibul H. M.; Stebbins C. C. *Physical and Thermodynamic Properties of Pure Chemicals*. *Data Compilations*; Taylor & Francis: Bristol, UK, 1989−2004.
(32) Polishuk, I.; Wisniak, J.; Segura, H. *Chem Eng. Sci.* **2001**, *56*, 6485.
(33) Younglove, B. A.; Ely, J. F. *J. Phys. Chem. Ref. Data* **1987**, *16*, 577.
(34) Das, T. R.; Reed, C. O., Jr.; Eubank, P. T. *J. Chem. D* **1977**, *22*, 3.
(35) Stephan, K.; Hildwein, H. *Recommended data of selected compounds and binary mixtures 1+2. Tables, diagrams and correlations*; DECHEMA: Stuttgart, Germany, 1987.
(36) Perry, R. H.; Green, D. W. *Perry's Chemical Engineers' Handbook*, 7th ed.; McGraw-Hill: New York, 1997.
(37) Orbey, H.; Vera, J. H. *AIChE J.* **1983**, *29*, 107.
(38) Kowalska, T.; Podgorny, A. *Chromotographia* **1991**, *31*, 387.
(39) Sage, B. H.; Reamer, H. H.; Olds, R. H.; Lacey, W. N. *Ind. Eng. Chem.* **1942**, *34*, 1108.
(40) Chen, R. J. J.; Chappelear, P. S.; Kobayashi, R. *J. Chem. Eng. D* **1978**, *19*, 58.